FUDMA Journal of Sciences (FJS)
ISSN online: 2616-1370
ISSN print: 2645 - 2944
Vol. 10 No. 23, December, 2026, pp 260 – 276
DOI: https://doi.org/10.33003/fjs-2026-1023-4970

Mango (*Mangifera indica* L.) Leaf Powder and Its Activated Carbon for Direct Black 168 Dye Removal: A Comparative Adsorption Study

[1]Modupe Munirat Adeyemi, *[1]Mojeed Oluwasegun Kasim, [1]David D. Nabaida, [2]Habib Isa Adamu and [2]Benjamin Barnabas Tagang

[1]Department of Chemistry, Faculty of Science, Nigerian Defence Academy, Kaduna, Nigeria.
[2]Department of Pure and Applied Chemistry, Faculty of Physical Sciences, Kaduna State University, Kaduna, Nigeria.

*Corresponding authors' email: kasimmojeed747@gmail.com

Received: 27 July 2026
Accepted: 19 Oct. 2026
Published: 17 Nov. 2026

ABSTRACT
The discharge of dye-laden effluents from tannery industries represents a major environmental challenge due to their persistence, toxicity, and resistance to biodegradation. Developing low-cost, sustainable adsorbents is therefore critical for effective wastewater treatment. This study comparatively evaluated the adsorption performance of mango leaf powder (MLP) and mango leaf-derived activated carbon (ML-AC) for the removal of Direct Black 168 dye from aqueous solutions. Batch adsorption experiments were conducted to investigate the effects of solution pH, adsorbent dosage, initial dye concentration, and contact time. Maximum dye removal was achieved at pH 2 for both adsorbents, with optimum adsorbent dosages of 0.75 g for MLP and 0.35 g for ML-AC, while equilibrium was attained after 120 min and 80 min, respectively. Under these optimized adsorption conditions, MLP and ML-AC achieved dye removal efficiencies of 75.66% and 78.34%, corresponding to experimental equilibrium adsorption capacities (q_e) of 10.09 mg/g and 22.38 mg/g, respectively at an initial dye concentration of 100 mg/L. The equilibrium data were best described by the Freundlich isotherm, indicating multilayer adsorption on heterogeneous surfaces. The adsorption kinetics were best fitted by the pseudo-second-order model, suggesting that chemisorption may have contributed to the adsorption process. The study demonstrates that both mango leaf powder and mango leaf-derived activated carbon are potential sustainable adsorbents for the removal of Direct Black 168 from aqueous solution, with phosphoric acid activation improving the adsorption performance of the mango leaf powder under the investigated conditions.

Keywords: Adsorption, Direct Black 168, Isotherm, Kinetics, *Mangifera indica*, Activated Carbon

INTRODUCTION

Synthetic dyes are among the most hazardous contaminants discharged in industrial effluents due to their complex aromatic and azo structures, which impart high chemical stability and resistance to biodegradation (Attallah et al., 2016; Aragaw, 2024). Their widespread use in textile, leather, paper, plastic, rubber, cosmetic, pharmaceutical, and food industries generates large volumes of coloured wastewater that pose serious environmental and public health concerns (Murugan et al., 2010). Besides their aesthetic impact, dyes reduce light penetration in aquatic systems, impair photosynthesis, increase biological oxygen demand, and decrease dissolved oxygen levels, thereby threatening aquatic ecosystems (Inbaraj & Chen, 2011). Moreover, many synthetic dyes exhibit toxic, mutagenic, and carcinogenic properties, making their removal from industrial wastewater an important environmental priority (Attallah et al., 2016).

The leather industry is one of the major contributors to dye-containing wastewater. During the wet finishing stage of leather processing, dyes are applied in aqueous media to impart uniform surface and internal coloration. This process generates substantial volumes of highly coloured wastewater containing residual dyes and auxiliary chemicals. In addition to visual pollution, dye-contaminated effluents reduce the reoxygenation capacity of receiving water bodies, exhibit acute and chronic toxicity, hinder biological wastewater treatment, and limit water reuse within industrial processes (Piccin et al., 2009; Gao et al., 2010).

Several treatment technologies have been developed for dye removal, including ion exchange, membrane filtration, advanced oxidation processes, solvent extraction, coagulation, and adsorption (Ali et al., 2021). Among these techniques, adsorption remains one of the most effective and economically viable methods because of its simplicity, high removal efficiency, low operating cost, ease of operation, and the possibility of adsorbent regeneration (Ghoreishi & Haghighi, 2003). Consequently, considerable attention has been directed toward developing inexpensive and sustainable adsorbents from agricultural residues and other biomass resources.

Agricultural wastes have attracted increasing interest as alternative adsorbents because they are inexpensive, abundant, renewable, and often require minimal processing before use (Crini, 2006). Many lignocellulosic materials possess appreciable adsorption capacities and relatively fast adsorption kinetics, making them attractive substitutes for commercial activated carbon (Crini, 2006). Adsorption performance is influenced by several operational parameters, particularly solution pH, which affects both the surface charge of the adsorbent and the ionization state of the adsorbate (Salleh et al., 2011). In general, untreated agricultural wastes have been reported to exhibit greater affinity for cationic dyes than for anionic dyes (Salleh et al., 2011).

Several agricultural by-products have demonstrated promising adsorption performance. *Annona squamosa* seeds have been successfully employed as low-cost adsorbents for removing cationic dyes, with adsorption strongly influenced

by solution pH (Santhi et al., 2016). Similarly, sawdust, an abundant lignocellulosic waste, has been extensively investigated as a precursor for activated carbon because of its high cellulose content, large surface area after activation, and well-developed microporous structure (Matos et al., 2011; M'Hamdi et al., 2016; Chikri et al., 2020). Activated carbons prepared from sawdust have demonstrated excellent adsorption capacities for a wide range of dyes in aqueous solutions (Chikri et al., 2020).

Among lignocellulosic biomaterials, mango (*Mangifera indica* L.) leaves have emerged as promising low-cost adsorbents due to their abundance and rich surface functional groups. Mango trees are widely distributed in tropical and subtropical regions and belong to the family *Anacardiaceae* (Lizada, 1993). Large quantities of mango leaves are generated annually as agricultural waste and are commonly discarded or openly burned, contributing to environmental pollution. Their conversion into adsorbent materials therefore offers both environmental and economic benefits (Murugan et al., 2010).

Previous studies have demonstrated the adsorption potential of mango leaf powder (MLP) for dye removal. Murugan et al. (2010) reported that MLP effectively removed Grey BL dye from aqueous solution, with adsorption being strongly influenced by solution pH. The equilibrium data were adequately described by both Langmuir and Freundlich isotherms, while the adsorption kinetics followed the pseudo-first-order model. Similarly, Ibrahim and Jimoh (2019) investigated the adsorption of Rhodamine B onto mango leaf powder and reported a maximum removal efficiency of 87%. The adsorption process followed the pseudo-second-order kinetic model, while the Freundlich isotherm provided the best description of the equilibrium data, indicating multilayer adsorption on a heterogeneous surface.

Direct Black 168 is a synthetic direct azo dye containing multiple azo linkages and sulfonate groups. The presence of sulfonate groups contributes to its anionic character and water solubility. Direct Blak 168 has molecular formula of $C_{34}H_{24}N_9Na_3O_{11}S_3$ and a molecular weight of 899.8 g/mol (National Center for Biotechnology Information [NCBI], 2026). The presence of sulfonate groups contributes to its anionic and water-soluble nature, while its relatively large molecular structure may influence its interaction with adsorbent surfaces and accessibility to adsorption sites. These structural characteristics make its removal from aqueous media an important consideration in the treatment of dye-containing wastewater.

Despite these encouraging findings, previous investigations have largely focused on laboratory dyes or heavy metal ions. Studies evaluating the adsorption performance of mango leaf powder and mango leaf-derived activated carbon for industrial dyes remain limited. Furthermore, comparative investigations assessing the performance of the raw biomass and its activated carbon derivative under identical experimental conditions are scarce. To the best of our knowledge, no published study has systematically compared mango leaf powder and mango leaf-derived activated carbon for the adsorption of Direct Black 168 dye from aqueous solution. Such a comparison is important for determining whether chemical activation provides a measurable improvement in adsorption performance over the untreated biomass and for identifying the more effective adsorbent under the investigated conditions.

Direct Black 168 is a widely used azo dye in the leather and textile industries, and its persistence, toxicity, and resistance to biodegradation make it a significant environmental pollutant. Therefore, developing efficient and sustainable adsorbents for its removal is of considerable practical importance.

Accordingly, this study aimed to compare the adsorption performance of mango leaf powder (MLP) and mango leaf-activated carbon (ML-AC) for the removal of Direct Black 168 dye from aqueous solution under batch conditions. Specifically, the study sought to (i) prepare MLP and ML-AC adsorbents, (ii) investigate the effects of operational parameters including solution pH, adsorbent dosage, initial dye concentration, and contact time on adsorption efficiency, and (iii) elucidate the adsorption mechanism using equilibrium isotherm and kinetic models.

MATERIALS AND METHODS

Materials

Industrial-grade Direct Black 168 dye (C.I. 335475; CAS: 85631-88-5; $C_{34}H_{24}N_9Na_3O_{11}S_3$, 899.8 g/mol), hydrochloric acid (HCl), sodium hydroxide (NaOH), and phosphoric acid (H_3PO_4) were used without further purification. Distilled water was employed for all solution preparations. Fresh mango (*Mangifera indica* L.) leaves for this study were collected from local fields in Sabon Tasha, Kaduna. Authentication of the leaves was carried out at the Herbarium section of the Department of Biology, Kaduna State University, Kaduna and given a voucher number: KASU/BSH/1678.

Preparation of Adsorbents

Mango Leaf Powder (MLP): Leaves were oven-dried at 80 °C until constant weight was achieved, ground, and sieved to 300 µm. To remove coloring matter, 100 g of powder was boiled in distilled water at 100 °C, filtered, oven-dried again, and stored in airtight containers (Ibrahim & Jimoh, 2019).

Mango Leaf–Activated Carbon (ML-AC): MLP was impregnated with 40% H_3PO_4 (1:2 ratio) at 80 °C for 12 h, carbonized in a closed muffle furnace with limited air supply at 500 °C for 1.5 h, cooled, washed with 0.1 M NaOH and distilled water until neutral pH, oven-dried at 105 °C, sieved to 300 µm, and stored (Chikri et al., 2020). Phosphoric acid (H_3PO_4) was selected as the activating agent because of its established effectiveness in the chemical activation of lignocellulosic biomass. It promotes the breakdown and cross-linking of biomass components, facilitating pore development, and is capable of producing activated carbons at relatively lower activation temperatures and shorter processing times than conventional physical activation, with comparatively high carbon yields and the development of surface functional groups that may enhance adsorption performance (Neme et al., 2022; Sirajoa & Zainia, 2023).

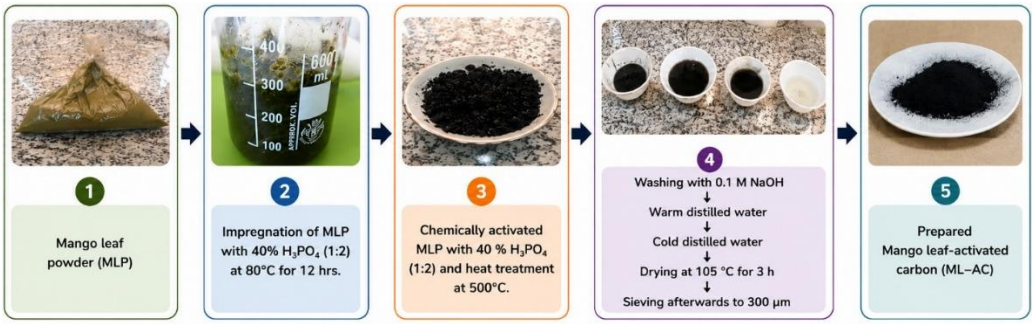


Figure 1: Diagram for the Chemical Activation Process of Mango Leaf Powder-Derived Activated Carbon

Preparation of Dye Solution

The dye, Direct Black 168 was supplied by the Tannery Unit of the Nigerian Institute of Leather and Science Technology (NILEST) Samaru, Zaria, Kaduna state, Nigeria. A 1000 mg L^{-1} stock solution of the dye was prepared by dissolving 1 g dye in 1 L distilled water. Working solutions were obtained by serial dilution using:

$$C_o \times V_o = C_d \times V_d \quad (1)$$

Where, C_0 and V_0 are the stock concentration and volume, and C_d and V_d are the desired concentration and final volume (Idan et al., 2018; Kolawole et al., 2022).

Calibration Curve Preparation

A calibration curve for the dye was prepared at λ_{max} = 607 nm and used to determine the concentration of the dye during the adsorption studies. The dye concentrations over the range (0 - 400 mg/L) were prepared from the stock solution (1000 mg/L) and their respective absorbance values were read on a UV-Vis spectrophotometer. A calibration curve of absorbance against dye concentrations was plotted (Emmanuel et al., 2009).

The linear equation obtained from Beer – Lambert's law (Skoog et al., 2014):

$$A = mC + b \quad (2)$$

Where, A = measure absorbance, C = Concentration of the analyte (mg/L), m = slope of the calibration line, b = y–intercept

The calibration equation obtained from the plot of absorbance vs dye concentration:

$$y = 0.0056x + 0.1337 \quad (3)$$

By substituting the calibration equation into the linear equation from Beer – Lambert's law:

$$A = 0.0056C + 0.1337 \quad (4)$$

All concentrations in this study were calculated using the equation below:

$$C = \frac{A - 0.1337}{0.0056} \quad (5)$$

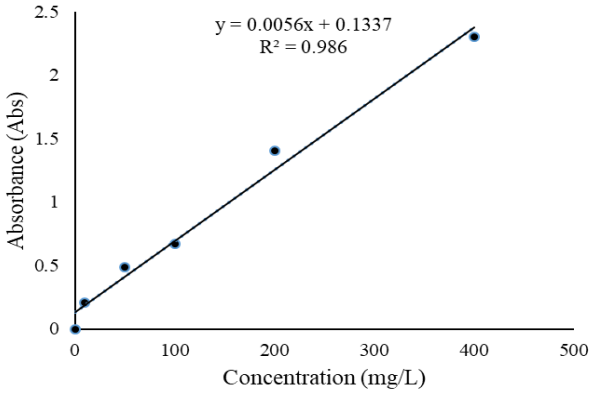


Figure 2: Calibration Curve of Direct Black 168 Dye: Absorbance vs. Concentration

Batch Adsorption Experiments

Adsorption was conducted in 250 mL plastic Erlenmeyer flasks with 100 mL dye solution, shaken in an orbital flask shaker at 25 ± 2 °C (350 revolutions per minute). At the end of adsorption tests, samples were centrifuged and the concentration of residual dye in the supernatant solution was analyzed using a UV/VIS spectrophotometer (Model: Jenway 6305 spectrophotometer) at λmax = 607 nm (Murugan et al., 2010).

The adsorption capacity (q_e) and percentage removal (R%) were calculated as:

$$q_e = \frac{(C_0 - C_e)V}{m}, \quad (6)$$

$$R\% = \frac{C_0 - C_e}{C_0} \times 100 \quad (7)$$

Where, C_0 = initial dye concentration (mg L^{-1}), C_e= equilibrium dye concentration (mg L^{-1}), V= solution volume (L), and m = adsorbent mass (g).

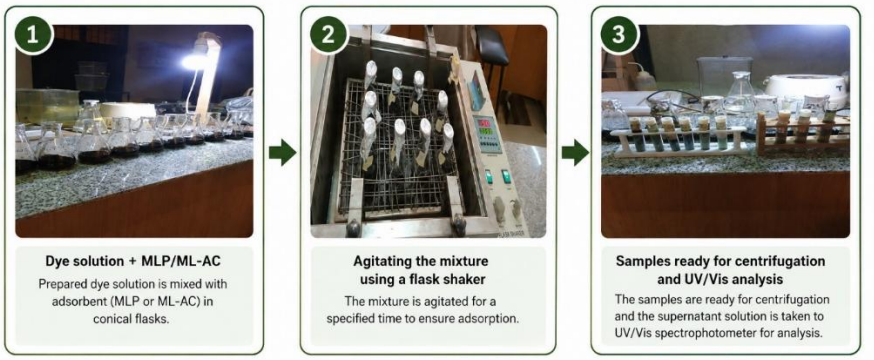


Figure 3: Batch Adsorption of Direct Black 168 Dye

Experimental Design

The adsorption experiments were conducted using one-factor-at-a-time (OFAT) experimental approach to investigate the effects of pH, adsorbent dose, initial dye concentration, and contact time on the removal of Direct Black 168 from aqueous solution. In each experiment, one experimental variable was varied while the other operating conditions were kept constant. The optimum condition obtained from each preceding experiment was subsequently used in the next experiment.

Effect of Operational Parameters

Solution pH

The effect of pH on the removal of the dye was investigated over the range pH 2 - 10. The pH was adjusted with 0.1M NaOH and 0.1M HCl solutions. In this study, 100 ml of the dye solution with a concentration of 100 mg/L was taken in a plastic Erlenmeyer flask and agitated with the 0.5 g of Mango Leaf Powder for 2 hours. A similar procedure was carried out separately for Mango leaf – activated carbon (Uddin et al., 2017).

Adsorbent Dosage

The effect of adsorbent dose was studied at the optimum pH previously obtained, by contacting 100 ml dye solution of initial concentration 100 mg/L with different amounts of MLP (0.55 - 0.95 g) while ML-AC (0.25 - 0.55 g) was contacted separately for a contact time of 2 hours till an equilibrium was attained, which were the optimum dosage, these values were chosen for subsequent experiments (Uddin et al., 2017; Murugan et al., 2010).

Initial Dye Concentration

This was investigated at initial concentrations of 100 - 350 mg/L under the optimum pH and optimum adsorbent dose. For the experiment using mango leaf powder, 100 mL of the dye solutions of different initial concentrations were placed in separate flasks and agitated with the optimum adsorbent dose previously obtained for 2 hours. A similar procedure was conducted for mango-leaf activated carbon (Uddin et al., 2017).

Contact Time

This was investigated over different contact times of 5 - 140 minutes using the optimum pH, adsorbent dose, and initial dye concentration established in the preceding optimization experiments. For MLP, 100 mL of the dye solution with initial concentration of 100 mg/L was agitated with the optimum adsorbent dose. At predetermined time intervals (5 – 140 min), and the samples were collected for analysis. A similar procedure was carried out separately for mango-leaf activated carbon. The equilibrium contact time was then extrapolated at the maximum adsorption (Uddin et al., 2017).

Adsorption Isotherms

Adsorption equilibrium isotherm was performed in a set of Erlenmeyer flasks (250 mL) where 100 mL solutions of dye at different initial concentrations (100 - 350 mg/L) were placed in these flasks. Equal optimum mass of mango leaf powder was added to the dye solutions and agitated at a temperature of (25 ± 2°C) for 4 hours to ensure equilibrium. After equilibrium was reached, the concentrations in the samples were analyzed as before. A similar procedure was carried out separately for mango-leaf activated carbon (Uddin et al., 2017). The models for analyzing equilibrium adsorption data included, the Langmuir, Freundlich, Temkin, and Dubinin - Radushkevich models (Khayyun & Mseer, 2019; Satish et al., 2012; Ibrahim & Jimoh, 2019).

The linear form of the Langmuir isotherm equation (monolayer adsorption on homogeneous sites) is given as:

$$\frac{C_e}{q_e} = \frac{1}{q_{max} K_L} + \frac{C_e}{q_{max}} \quad (8)$$

Where, q_e is the amount of adsorbate adsorbed at equilibrium (mg/g), q_{max} is the maximum (monolayer) adsorption capacity (mg/g), C_e is the equilibrium concentration of adsorbate in solution (mg/L), K_L is the Langmuir adsorption constant (L/mg). Where q_{max} is monolayer (maximum) adsorption capacity (mg/g) and K_L is Langmuir constant related to energy of adsorption (L/mg) obtained from the slope and intercept values of the plot C_e/q_e against C_e respectively.

The Separation Factor (Dimensionless Constant) (R_L) is given as:

$$R_L = \frac{1}{1 + K_L C_0} \quad (9)$$

Where, C_0 is the initial dye concentration (mg/L), K_L is the Langmuir constant (L/mg).

If,

$R_L > 1$ (Unfavorable adsorption), $R_L = 1$ (Linear adsorption), $R_L = 0$ (Irreversible adsorption),

$0 < R_L < 1$ (Favorable adsorption)

The linear form of the Freundlich isotherm equation (multilayer adsorption on heterogeneous surfaces) is given as:

$$Log\ q_e = Log\ K_F + \frac{1}{n} Log\ C_e \quad (10)$$

Where, q_e is the amount of adsorbate adsorbed at equilibrium (mg/g), C_e is the equilibrium concentration of adsorbate in solution (mg/L), K_F is the Freundlich constant $(mg/g)(L/mg)^{1/n}$, n is the adsorption intensity. A plot of log q_e against log C_e gives a straight line, K_F and n are constant incorporating factors affecting the adsorption capacity and intensity of adsorption calculated from the intercept and slope of the plot respectively.

The linear form of the Temkin isotherm equation (adsorbent–adsorbate interactions, linear heat decrease) is given as:

$q_e = B \ln A + B \ln C_e$ (11)

Where, q_e is the equilibrium adsorption capacity (mg/g), C_e is the equilibrium concentration of adsorbate in solution (mg/L). A is the Temkin equilibrium binding constant (L/mg) and B is the Temkin constant related to the heat of adsorption (mg/g) calculated from the intercept and slope of the plot q_e against ln C_e respectively (Satish et al., 2012).

The linear form of the Dubinin - Radushkevich isotherm equation (distinguishes physical vs. chemical adsorption) is given as:

$\ln q_e = \ln q_m - \beta \varepsilon^2$ (12)

Where, qe is the equilibrium adsorption capacity (mg/g), qm is the theoretical maximum adsorption capacity (mg/g), ε is the Polanyi potential (kJ/mol), β (mol^2/kJ^2) is the D-R isotherm constant related to mean free adsorption energy E ($kJmol^{-1}$). The values of β and q_m are gotten from the slope and intercept of the plot of In q_e against ε^2 respectively.

Expression of Polanyi potential is given as:

$$\varepsilon = RT\, In \left(1 + \frac{1}{C_e}\right) \quad (13)$$

Where, ε is the Polanyi potential (kJ/mol), R is the universal gas constant (0.008314 kJ mol^{-1} K^{-1}), T is the absolute temperature (K), C_e is the equilibrium concentration of adsorbate.

Expression of the mean free adsorption energy is given as:

$$E = \frac{1}{\sqrt{2\beta}} \quad (14)$$

Where, E is the mean free adsorption energy (kJ/mol), β is the D-R isotherm constant related to mean free adsorption energy (mol^2/kJ^2).

If,

E < 8 kJ/mol (physisorption), 8 – 16 kJ/mol (ion-exchange or mixed adsorption), E > 16 kJ/mol (chemisorption)

(Ibrahim & Jimoh, 2019)

Adsorption Kinetics

Adsorption kinetic experiment was carried out by agitating 100 mL of dye solutions of different initial concentrations of 100 - 350 mg/L with the optimum dose of MLP in a 250 ml plastic Erlenmeyer flask at a temperature of (25 ± 2°C). The aqueous samples were taken over different contact times of 5 - 260 minutes, centrifuged and the residual concentration of the dye in the supernatant solution was analyzed as before. A similar procedure was carried out separately for mango-leaf activated carbon (Uddin et al., 2017). The Lagergren's pseudo-first-order and pseudo-second-order kinetic models were used (Lagergren, 1898; Ho & Mckay, 1999).

The Lagergen pseudo-first-order kinetic equation is given as:

$$Log\,(q_e - q_t) = Log\, q_e - \frac{K_1}{2.303} t \quad (15)$$

Where, q_t is the amount of adsorbate adsorbed at time t (mg/g), q_e is the amount of adsorbate adsorbed at equilibrium (mg/g), t is the time of adsorption (min), k_1 is the Pseudo-first-order rate constant (min^{-1}). The slope and intercept values of plot log ($q_e - q_t$) against t, used to determine pseudo first order rate constant (k_1) and calculated amount of dye adsorbed per unit mass of adsorbent $q_{e(cal)}$ respectively.

The Lagergen pseudo-second-order kinetic equation is given as:

$$\frac{t}{q_t} = \frac{1}{K_2\, q_e^2} + \frac{t}{q_e} \quad (16)$$

Where, q_t is the amount of adsorbate adsorbed at time t (mg/g), q_e is the amount of adsorbate adsorbed at equilibrium (mg/g), t is the time of adsorption (min), k_2 is the Pseudo-second-order rate constant (g/mg.min). The slope and intercept of plot of t/qt against t, gives values of $q_{e(cal)}$ and k_2 respectively.

Data Analysis

Model fit was evaluated using coefficient of determination, R^2 values. Statistical analysis was performed using OriginPro and Excel, with significance set at $p < 0.05$.

RESULTS AND DISCUSSION

Effect of Operational Parameters on the Adsorption of Direct Black 168 Dye

The adsorption performance of mango leaf powder (MLP) and mango leaf-derived activated carbon (ML-AC) was evaluated under varying operational parameters, including solution pH, adsorbent dosage, initial dye concentration, and contact time. Understanding their effects is essential for optimizing adsorption efficiency.

Effect of pH

The effect of solution pH on the adsorption of Direct Black 168 dye by MLP and ML-AC is presented in Figures 4 and 5. For mango leaf powder, dye removal decreased from 77.45 % at pH 2 to 13.16 % at pH 10, while ML-AC showed a similar decline from 79.23 % to 11.02 % over the same range. The optimum pH for both adsorbents was 2. At acidic pH values, the adsorbent surfaces are positively charged, favoring electrostatic attraction with the anionic dye molecules. While the electrostatic attraction is favorable at pH 2, the presence of excess H^+ ions may compete with dye molecules for active sites, reducing the overall removal efficiency. As the solution pH increased, deprotonation of the adsorbent surface reduced positive charge density, thereby diminishing adsorption efficiency.

The observed pH-dependent behavior highlights the critical role of solution chemistry in adsorption processes. Previous studies on agricultural waste-derived adsorbents have reported maximum adsorption of anionic dyes to occur under acidic conditions (Elwakeel et al., 2020; Guiza et al., 2018; Garg et al., 2003). Malik (2003) similarly reported that sawdust-based activated carbons removed Acid Yellow 36 more efficiently at pH 2.

The solution pH was found to be one of the most influential parameters governing dye adsorption. The superior performance of ML-AC compared with MLP across the investigated pH range can be attributed to phosphoric acid activation, which can promote dehydration, condensation, and cross-linking, and pore development during thermal treatment (Danish & Ahmad, 2018; Zuo et al., 2010).

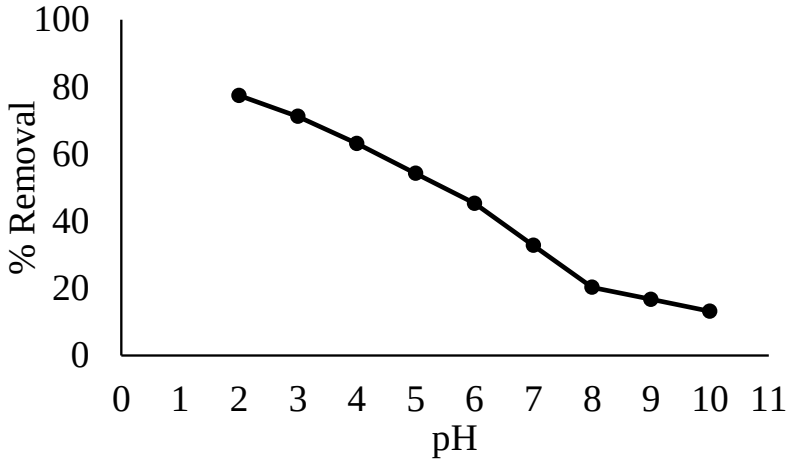


Figure 4: Effect of pH on the Adsorption of Direct Black 168 Dye Onto Mango Leaf Powder (C_o = 100 mg/L, W = 0.5 g, V = 100 mL)

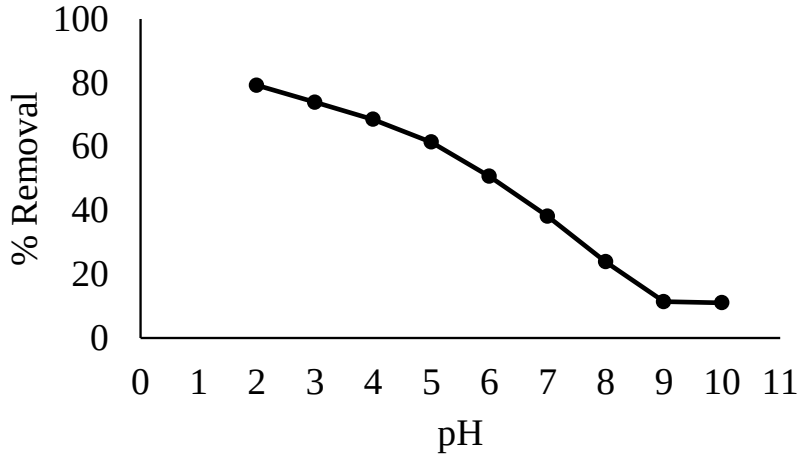


Figure 5: Effect of pH on the Adsorption of Direct Black 168 Dye onto Mango Leaf – Activated Carbon (C_o = 100 mg/L, W = 0.5 g, V = 100 mL)

Effect of Adsorbent Dose

The influence of adsorbent dosage on the removal of Direct Black 168 dye is presented in Figures 6 and 7. For mango leaf powder (MLP), dye removal increased from 59.52% at 0.55 g to 75.77% at 0.95 g, with an optimum dosage of 0.75 g. Beyond this dosage, further increases produced only marginal improvements. For mango leaf-derived activated carbon (ML-AC), removal rose from 66.16% at 0.25 g to 85.27% at 0.55 g, with an optimum dosage of 0.35 g. Similar to MLP, efficiency plateaued beyond the optimum dosage. This could result from overlapping effects, including increased adsorbent-adsorbent interactions, aggregation, overlap of adsorption sites.

The observed increase in removal efficiency with dosage is attributed to the greater number of adsorption sites available as adsorbent mass increases, thereby enhancing the probability of dye–adsorbent interactions (Salleh et al., 2011). However, once equilibrium is reached, additional adsorbent does not significantly improve removal because the dye concentration becomes limiting relative to the adsorbent mass. Therefore, the plateau in removal efficiency at higher adsorbent doses can be attributed to (i) site overlap and aggregation, (ii) the limited dye concentration becoming the restricting factor, or a combination of both. Because particle aggregation was not directly measured in the present study, the plateau is considered to result from a combination of these possible effects rather than being attributed solely to aggregation.

ML-AC consistently exhibited higher dye removal than MLP across the investigated dosage range, this superior performance is consistent with the enhanced adsorption characteristics imparted by phosphoric acid activation (Danish & Ahmad, 2018; Zuo et al., 2010). These findings are in agreement with previous studies, where optimum dosages were reported for mango leaf powder on Grey BL dye by Murugan et al. (2010), *Veronia amygdalina* leaf powder on Congo red by Zewde and Geremew (2022), and activated mango leaf powder on Congo red (Adelaja et al., 2019).

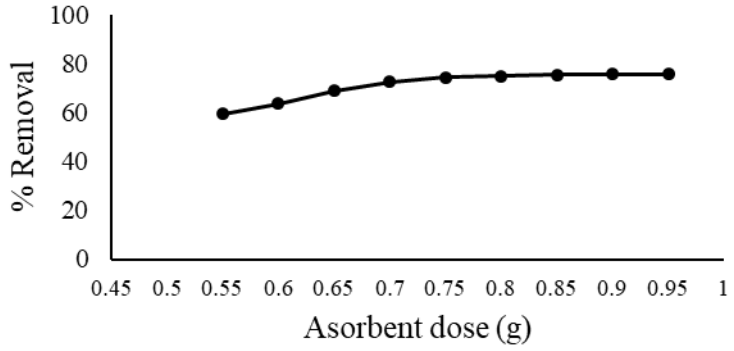


Figure 6: Effect of Adsorbent Dose on the Adsorption of Direct Black 168 Dye onto Mango Leaf Powder (C_o = 100 mg/L, V = 100 mL)

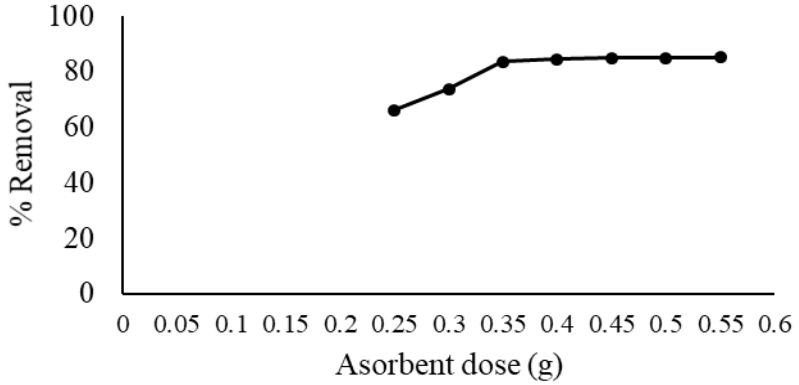


Figure 7: Effect of Adsorbent Dose on the Adsorption of Direct Black 168 Dye onto Mango Leaf – activated Carbon (C_o = 100 mg/L, V = 100 mL)

Effect of Initial Dye Concentration

The effect of initial dye concentration on the adsorption of Direct Black 168 dye by MLP and ML-AC is presented in Figures 8 and 9. For mango leaf powder, dye removal decreased from 76.25 % at 100 mg L^{-1} to 65.25 % at 350 mg L^{-1}, while ML-AC showed a similar decline from 77.45 % to 67.03 % over the same concentration range. Although percentage removal decreased with increasing dye concentration, the adsorption capacity increased due to the stronger concentration gradient between the solution and the adsorbent surface, which provided a greater driving force for mass transfer of dye molecules from the bulk solution toward available adsorption site (Uddin et al., 2017).

The decrease in percentage removal with increasing initial dye concentration can be attributed primarily to the fixed adsorbent dosage and finite number of available adsorption sites relative to the increasing amount of dye in solution (Salleh et al., 2011). This explains the decline in percentage removal at higher concentrations despite the increase in adsorption capacity.

The higher adsorption performance of ML-AC is consistent with the established effects of phosphoric acid activation on lignocellulosic precursors (Danish & Ahmad, 2018; Loannidou & Zabaniotou, 2007). These findings are consistent with previous studies on lignocellulosic adsorbents, which reported similar trends of increasing adsorption capacity but decreasing percentage removal at higher dye concentrations due to site saturation (Son et al., 2016; Salleh et al., 2011; Chikri et al., 2020).

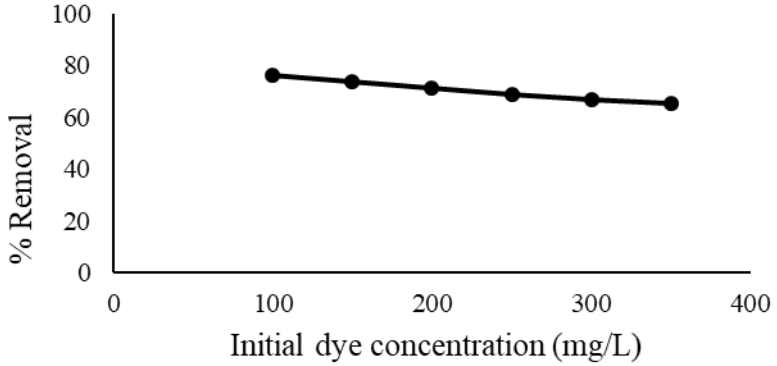


Figure 8: Effect of initial dye concentration on the adsorption of Direct Black 168 Dye onto Mango Leaf Powder (C_o = 100, 150, 200, 250, 300 and 350 mg/L, W = 0.75 g, V = 100 mL)

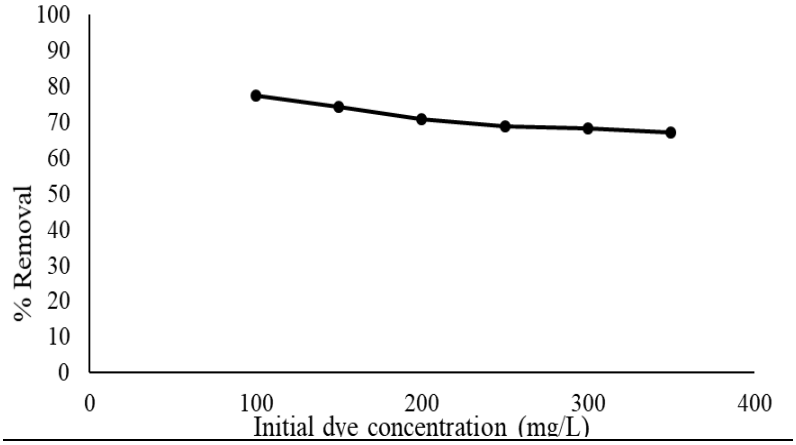


Figure 9: Effect of Initial Dye Concentration on the Adsorption of Direct Black 168 Dye onto Mango Leaf – activated Carbon (C_o = 100, 150, 200, 250, 300 and 350 mg/L, W = 0.35 g, V = 100 mL)

Effect of Contact Time

The effect of contact time on the adsorption of Direct Black 168 dye by MLP and ML-AC is presented in Figures 10 and 11. Under the optimized conditions, at the common initial dye concentration of 100 mg/L used for the contact time experiment, mango leaf powder adsorption increased rapidly within the first 30 min, reaching equilibrium in 120 min achieving 75.66% removal. In contrast, ML-AC adsorption increases rapidly within the first 20 min, and eventually exhibited a shorter equilibrium time of 80 min achieving 78.34% removal. The corresponding experimental adsorption capacities (q_e) at an initial dye concentration of 100 mg/L was 10.09 mg/g for MLP and 22.38 mg/g for ML-AC.

The rapid initial adsorption observed for both adsorbents can be attributed to the abundance of vacant surface sites. As adsorption progressed, the number of available sites decreased, resulting in a gradual reduction in the adsorption rate as the system approached equilibrium (Uddin et al., 2017). Beyond the equilibrium times, further increases in contact duration produced negligible changes in removal efficiency, indicating that dynamic equilibrium had been established between adsorption and desorption processes. The faster approach to equilibrium time and a higher experimental adsorption capacity observed for ML-AC is consistent with the structural modifications generally associated with phosphoric acid activation of lignocellulosic precursors (Danish & Ahmad, 2018; Loannidou & Zabaniotou, 2007).

These findings are consistent with previous studies, which reported similar adsorption behavior for agricultural waste-derived adsorbents. Khan et al. (2019) observed equilibrium at 160 min for mango leaf powder on Acid Yellow-99, while Yunus & Nuhu (2020) reported 90 min for rice husk activated carbon on Congo red, and Aminu et al. (2020) obtained 100 min for jujube seed carbon on Congo red. The observed trend reflects the general adsorption behaviour, characterized by rapid initial uptake due to abundant active sites, followed by a slower adsorption rate as these sites becomes progressively occupied and equilibrium is approached, as reported in previous studies (Adegoke et al., 2021).

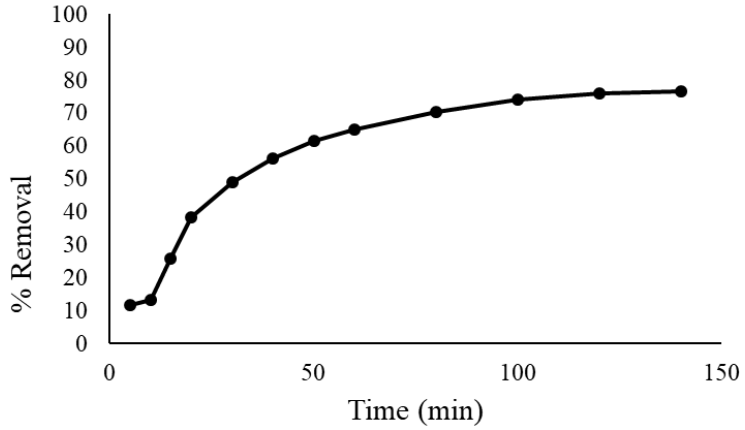


Figure 10: Effect of Contact Time on the Adsorption of Direct Black 168 onto Mango Leaf Powder (C_o = 100 mg/L, W = 0.75 g, V = 100 mL)

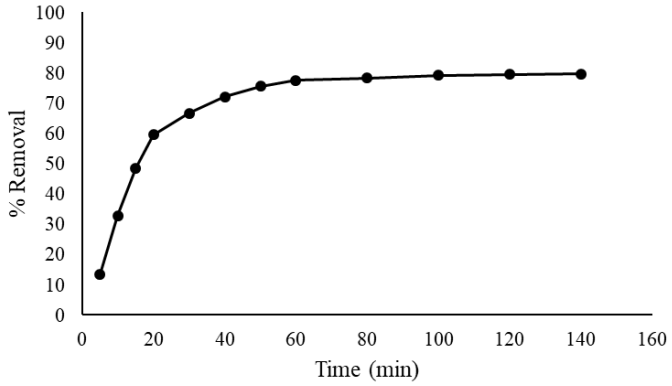


Figure 11: Effect of Contact Time on the Adsorption of Direct Black 168 Dye onto Mango Leaf – Activated Carbon (C_o = 100 mg/L, W = 0.35 g, V = 100 mL)

Adsorption Isotherm

The equilibrium adsorption data for Direct Black 168 dye were analyzed using Freundlich, Langmuir, Temkin, and Dubinin–Radushkevich (D–R) models. The isotherm parameters are presented in Tables 1 and 2 for mango leaf powder (MLP) and mango leaf–activated carbon (ML-AC), respectively.

Freundlich Isotherm

The Freundlich model provided the best fit for both adsorbents, with R^2 values of 0.9983 (MLP) and 0.9985 (ML-AC), indicating surface heterogeneity and multilayer adsorption. The adsorption intensity values (n > 1) suggested favorable adsorption, with n = 1.19 for MLP and n = 1.18 for ML-AC. These results are comparable to those reported by Ibrahim and Jimoh (2019) for Rhodamine B removal using mango leaf powder (n = 1.009) and Aminu et al. (2020) for jujube seed carbon on Congo red (n = 1.563). The Freundlich constant (K_F) was higher for ML-AC (2.32) than MLP (0.90), reflecting greater adsorption capacity following activation. Similar K_F values have been reported for activated rubber sawdust on methyl orange (K_F = 2.0854; Shining & Helen, 2022).

Langmuir Isotherm

The Langmuir model also showed good correlation (R^2 = 0.9959 for MLP; 0.9970 for ML-AC). For comparison with other adsorbents, the maximum monolayer adsorption capacity (q_{max}) for ML-AC (294.12 mg/g) is superior to the values reported for rubber seed activated carbon on Congo red (227.27 mg/g; Nizam et al., 2021), MLP for this study (142.86 mg/g), and ackee apple seeds on Congo red (161.89 mg/g; Bello et al., 2013). This enhanced capacity is attributed to chemical activation. The Langmuir binding affinity (K_L) was slightly higher for ML-AC (0.0055 L/mg) than MLP (0.0047 L/mg), indicating stronger dye–adsorbent interactions.

Temkin Isotherm

The Temkin constants further supported stronger adsorbate–adsorbent interactions for ML-AC. The binding constant (A) was 0.105 L/mg for ML-AC and 0.094 L/mg for MLP, indicating a slightly higher binding affinity of ML-AC for direct black 168. The Temkin constant (B), which is related to the variation in the heat of adsorption, was 39.08 mg/g for ML-AC and 17.99 mg/g for MLP. The higher B value for ML-AC suggests stronger adsorbate-adsorbent interactions and a greater change in adsorption energy with surface coverage. The difference in the Temkin parameters may be associated with changes in the surface characteristics and availability of adsorption sites following activation (Foo & Hameed, 2010).

Dubinin–Radushkevich (D–R) Isotherm

The relatively poor fit of the D-R isotherm (R^2 < 0.89) indicates that this model did not adequately describe the equilibrium data for the present adsorbents. The poor fit may reflect deviations from the model assumptions concerning the distribution of adsorption energies and the applicability of the model to the present aqueous adsorption system. This suggests that the adsorbent surface energy distribution is not homogeneous, and the assumption of a Gaussian energy distribution may not be appropriate for these heterogeneous adsorbents. The theoretical adsorption capacity (q_m) was higher for ML-AC (71.08 mg/g) than MLP (32.36 mg/g), indicating improved adsorption performance. The mean adsorption energy (E) values were 0.097 kJ/mol for ML-AC and 0.089 kJ/mol for MLP. The slightly higher E value for ML-AC suggests stronger adsorption interactions compared with MLP. These low E values are within the range commonly associated with physical adsorption in D-R analyses and therefore indicate that weak physical interactions may contribute substantially to the adsorption process. Similar low E values have been reported in previous adsorption studies; for example, an E values of 0.091 kJ/mol was reported for paraquat adsorption onto Ayous wood sawdust and was associated with physisorption process (Kamga, 2019). However, in addition to the model relatively poor agreement with the experimental data, also the E values alone are considered indicative rather than conclusive of the adsorption mechanism.

Among the models tested, the Freundlich isotherm provided the best fit for both adsorbents, this implies a multilayer adsorption on heterogeneous surfaces. The higher K_F, q_{max}, and Temkin constants for ML-AC indicate its stronger adsorption performance and greater affinity for Direct Black 168 under the conditions investigated. This difference is consistent with the established effects of phosphoric acid activation, which promotes dehydration, condensation, and cross-linking reactions during thermal treatment of lignocellulosic biomass and can facilitate pore development (Danish & Ahmad, 2018; Zuo et al., 2010).

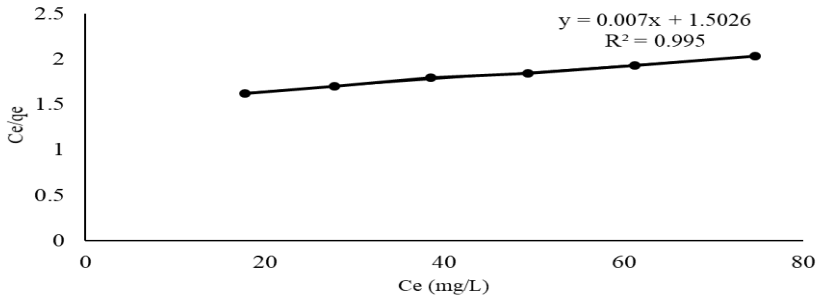


Figure 12: Langmuir isotherm for the adsorption of Direct Black 168Dye onto Mango leaf powder (C_0 = 100, 150, 200, 250, 300, and 350 mg/L, W = 0.75 g, V = 100 mL)

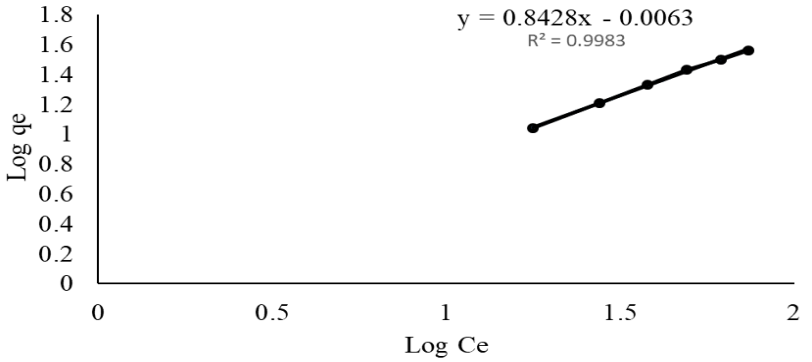


Figure 13: Freundlich Isotherm for the Adsorption of Direct Black 168Dye onto Mango Leaf Powder (C_0 = 100, 150, 200, 250, 300, and 350 mg/L, W = 0.75 g, V = 100 mL)

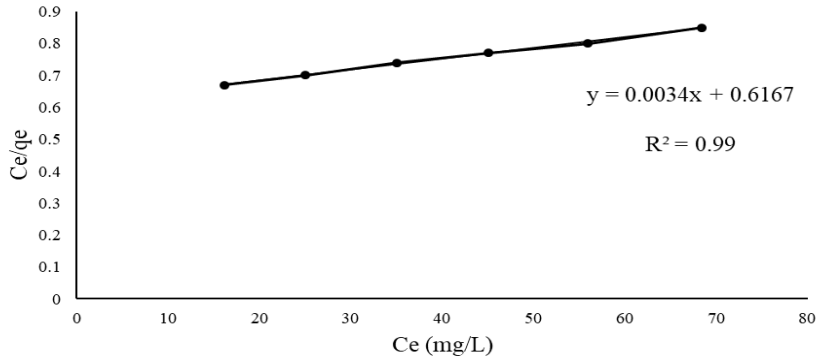


Figure 14: Langmuir Isotherm for the Adsorption of Direct Black 168Dye onto Mango leaf – activated Carbon (C_0 = 100, 150, 200, 250, 300, and 350 mg/L, W = 0.35 g, V = 100 mL)

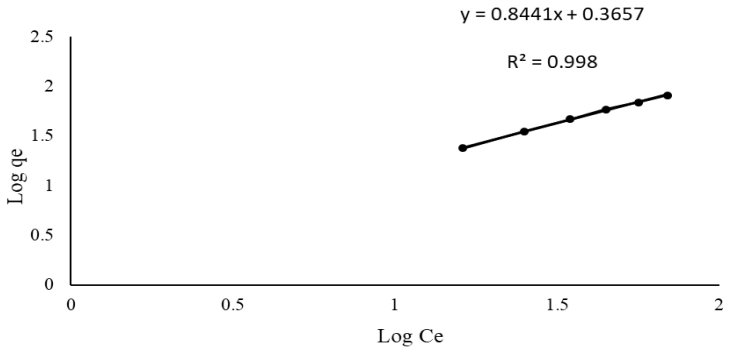


Figure 15: Freundlich Isotherm for the Adsorption of Direct Black 168Dye onto Mango leaf – Activated Carbon (C_0 = 100, 150, 200, 250, 300, and 350 mg/L, W = 0.35 g, V = 100 mL)

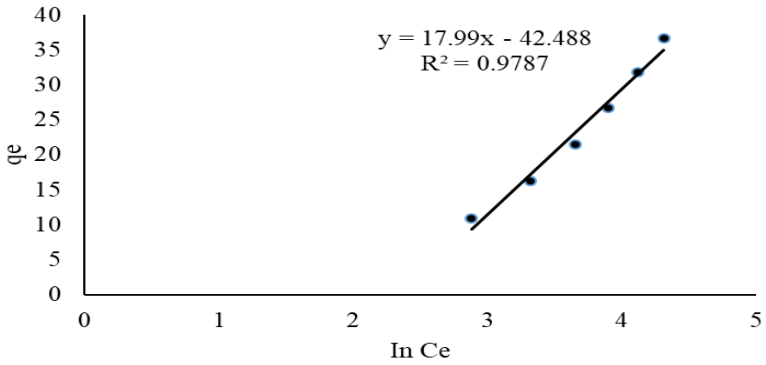


Figure 16: Temkin Isotherm for the Adsorption of Direct Black 168 Dye onto Mango leaf Powder (C_0 = 100, 150, 200, 250, 300, and 350 mg/L, W = 0.75 g, V = 100 mL)

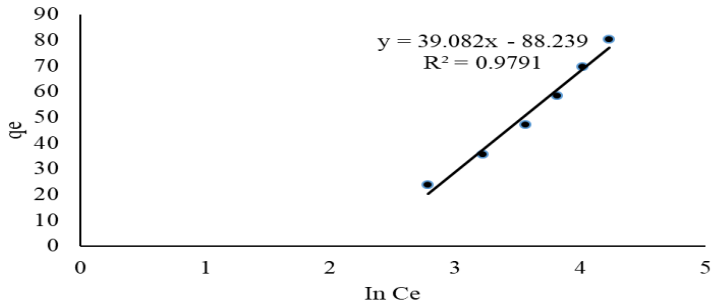


Figure 17: Temkin Isotherm for the Adsorption of Direct Black 168Dye onto Mango Leaf – Activated Carbon (C_0 = 100, 150, 200, 250, 300, and 350 mg/L, W = 0.35 g, V = 100 mL)

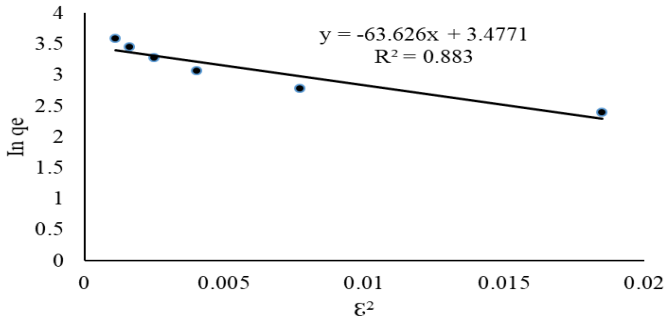


Figure 18: Dubinin-Radushkevich Isotherm for the Adsorption of Direct Black 168Dye onto Mango Leaf Powder (C_0 = 100, 150, 200, 250, 300, and 350 mg/L, W = 0.75 g, V = 100 mL)

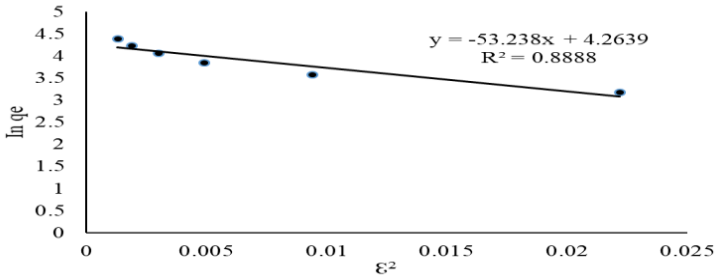


Figure 19: Dubinin-Radushkevich Isotherm for the Adsorption of Direct Black 168 Dye onto Mango Leaf – Activated Carbon (C_0 = 100, 150, 200, 250, 300, and 350 mg/L, W = 0.35 g, V = 100 mL)

All the isotherm parameters in table 1 and 2 were calculated from figure 12 to 19.

Table 1: Isotherm Parameters for the Adsorption of Direct Black 168 Dye by Mango Leaf Powder

Model	Parameter	Values
Freundlich	K_F (mg/g)/(L/mg)$^{1/n}$	0.9
	n	1.19
	R^2	0.9983
Langmuir	q_{max} (mg/g)	142.86
	K_L (L/mg)	0.0047
	R^2	0.9959
Temkin	A (L/mg)	0.094
	B (mg/g)	17.99
	R^2	0.9787
Dubinin -Radushkevich	q_m (mg/g)	32.36
	β (mol^{2}kJ^{-2})	63.626
	E (kJmol^{-1})	0.089
	R^2	0.883

Table 2: Isotherm Parameters for the Adsorption of Direct Black 168 Dye by Mango Leaf-Activated Carbon

Model	Parameter	Values
Freundlich	K_F (mg/g)/(L/mg)$^{1/n}$	2.32
	n	1.18
	R^2	0.9985
Langmuir	q_{max} (mg/g)	294.12
	K_L (L/mg)	0.0055
	R^2	0.9970
Temkin	A (L/mg)	0.105
	B (mg/g)	39.082
	R^2	0.9791
Dubinin -Radushkevich	q_m (mg/g)	71.08
	β (mol^{2}kJ^{-2})	53.238
	E (kJmol^{-1})	0.097
	R^2	0.8888

Separation Factor

The essential characteristics of the Langmuir isotherm can be expressed in terms of the dimensionless separation factor, R_L, (from equation 9) defined as:

$$R_L = \frac{1}{1+K_L C_0}$$

where K_L is the Langmuir constant (L/mg) and C_0 is the initial dye concentration (mg/L). The value of R_L indicates the nature of the adsorption process: unfavorable ($R_L>1$), linear ($R_L = 1$), favorable ($0 < R_L <1$), or irreversible ($R_L = 0$).

Tables 3 and 4 present the calculated R_L values for MLP and ML-AC at different initial dye concentrations (100–350 mg/L). For MLP, R_L decreased from 0.680 at 100 mg/L to 0.378 at 350 mg/L, while for ML-AC, values decreased from 0.645 to 0.342 over the same concentration range. The decreasing R_L values with increasing initial dye concentration indicate that the adsorption becomes progressively more favorable at higher concentrations, which is consistent with the Langmuir isotherm assumptions and reflects the stronger driving force for mass transfer.

Importantly, all R_L values for both adsorbents fall between 0 and 1, indicating that the adsorption of Direct Black 168 dye onto MLP and ML-AC was favorable across the investigated concentration range. These findings are consistent with previous reports, where separation factor values between 0 and 1 indicated favorable adsorption of dyes on various biosorbents (Satish et al., 2012; Uddin et al., 2017).

The separation factor analysis reinforces the suitability of both adsorbents for dye removal, with ML-AC exhibiting slightly lower R_L values than MLP, reflecting its stronger affinity and enhanced adsorption efficiency following chemical activation.

Table 3: Separation Factor (R_L) Calculated from Langmuir Constant (K_L) (0.0047 L/mg) for Mango Leaf Powder

Initial Concentration (mg/L)	R_L
100	0.680
150	0.587
200	0.515
250	0.460
300	0.415
350	0.378

Table 4: Separation Factor (R_L) calculated from Langmuir Constant (K_L) (0.0055 L/mg) for Mango Leaf – Activated Carbon

Initial Concentration (mg/L)	R_L
100	0.645
150	0.548
200	0.476
250	0.421
300	0.377
350	0.342

Adsorption Kinetics

Kinetic modeling provides insight into the rate and mechanism of solute uptake by adsorbents. In this study, the adsorption of Direct Black 168 dye onto mango leaf powder (MLP) and mango leaf–activated carbon (ML-AC) was analyzed using pseudo-first-order and pseudo-second-order models (Figures 19–22). The kinetic parameters derived from these models are summarized in Tables 5 and 6.

Pseudo-First-order Model

This model assumes that the rate of adsorption is proportional to the number of unoccupied sites on the adsorbent surface, a behavior typically associated with physisorption (Sangoremi, 2025). For both MLP and ML-AC, the correlation coefficients (R^2) obtained from the pseudo-first-order model were generally lower than those of the pseudo-second-order model. Moreover, the calculated adsorption capacities ($q_{e(cal)}$) showed poor agreement with the experimental values ($q_{e(exp)}$), indicating that this model did not adequately describe the adsorption process. The pseudo-first-order rate constant (k_1) decreased with increasing dye concentration, suggesting that higher concentrations led to stronger competition among dye molecules for limited adsorption sites. Similar trends have been reported by Satish et al. (2012).

Pseudo-Second-order Model

This model assumes that chemisorption is the rate-limiting step, involving valence forces through electron sharing or exchange between adsorbate and adsorbent (Ho & McKay, 1999). For both MLP and ML-AC, the pseudo-second-order model provided an excellent fit, with R^2 values approaching unity (0.998–1.000). The calculated adsorption capacities closely matched the experimental values across all concentrations, confirming the suitability of this model. The pseudo-second-order rate constant (k_2) increased with dye concentration up to 200–250 mg/L, reflecting the stronger driving force for mass transfer at higher concentration gradients. At higher concentrations, k_2 values plateaued or slightly declined, indicating progressive saturation of adsorption sites. Similar behavior has been observed in other studies (Neag et al., 2019). The pseudo-second-order rate constants (k_2) for ML-AC ranged from 0.0011 to 0.0057 g/mg·min, which were consistently higher than those for MLP (0.0012 to 0.0030 g/mg·min) at corresponding concentrations, indicating the faster adsorption kinetics of ML-AC.

Comparison of MLP and ML-AC

As seen from table 5, the correlation coefficients R^2 values obtained for pseudo-second-order were higher than those of the pseudo-first-order model. The pseudo-first-order model gave calculated q_e values that were significantly different from experimental values (e.g., for MLP at 300 mg/L, $q_{e(cal)}$ = 16.97 mg/g vs. q_e(exp)= 32.83 mg/g; Table 5), whereas the pseudo-second-order model gave values that closely matched the experimental data (34.25 mg/g vs. 32.83 mg/g, respectively, at the same initial concentration, 300 mg/L). This confirms that the pseudo-second-order model is superior, the results revealed that the pseudo second-order model was the best one in describing the kinetics of Direct Black 168 adsorbed onto mango leaf powder.

As seen from table 6, the correlation coefficients R^2 values obtained for pseudo-second-order were higher than those of the pseudo-first-order model. The pseudo-first-order model gave calculated q_e values that were significantly different from experimental values (e.g., for ML-AC at 250 mg/L, q_e(cal)= 14.08 mg/g vs. q_e(exp)= 57.38 mg/g; Table 6), whereas the pseudo-second-order model gave values that closely matched the experimental data (58.14 mg/g vs. 57.38 mg/g, respectively, at the same initial concentration, 250 mg/L). This confirms that the pseudo-second-order model is superior, the results revealed that the pseudo-second-order model was the best one in describing the kinetics of Direct Black 168 dye adsorbed onto mango leaf – activated carbon.

ML-AC reached equilibrium in a shorter time than MLP under the same experimental conditions. ML-AC consistently exhibited higher adsorption capacities compared with MLP. For example, at 250 mg/L, ML-AC achieved an experimental q_e of 57.38 mg/g compared with 27.27 mg/g for MLP. The higher adsorption performance of ML-AC is consistent with the established effects of phosphoric acid activation on lignocellulosic precursors (Danish & Ahmad, 2018; Loannidou & Zabaniotou, 2007). The results are consistent with previous reports, where activated carbons derived from agricultural wastes demonstrated improved adsorption kinetics and capacities compared with raw biomass (Ojedokun & Bello, 2017; Ibrahim & Jimoh, 2019).

The pseudo-second-order model best described the adsorption kinetics of Direct Black 168 dye onto both MLP and ML-AC, suggesting that chemisorption contributes to the adsorption mechanism. These findings are consistent with earlier studies on anionic dye removal using lignocellulosic materials (Ho & McKay, 1999).

Although ML-AC exhibited higher adsorption performance than MLP under the investigated conditions, its preparation involves additional processing steps, including chemical impregnation with H_3PO_4, thermal treatment 500ºC, and subsequent washing with NaOH. These additional processing requirements imply greater consumption of chemicals, water, and energy compared with the preparation of MLP. Therefore, for practical application, the choice between MLP and ML-AC would depend on the required treatment performance and the associated preparation and operating costs. MLP may offer an advantage where a simpler and less energy-intensive adsorbent preparation is preferred, whereas ML-AC may be advantageous where its improved adsorption performance justifies the additional processing requirements.

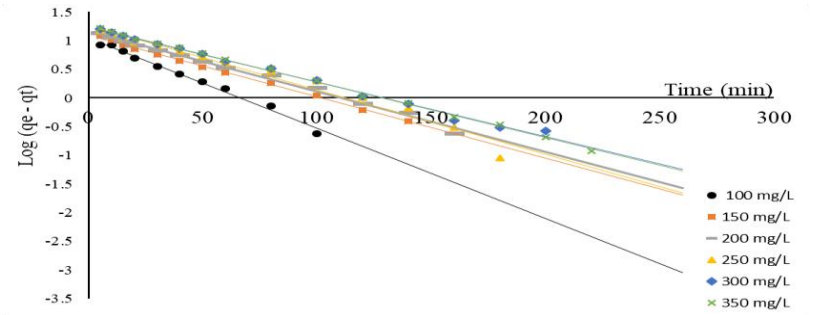


Figure 20: The pseudo-first-order Kinetic Plot for Adsorption of Direct Black 168Dye onto Mango Leaf Powder (C_0 = 100, 150, 200, 250, 300 & 350 mg/L, W = 0.75 g, V = 100 mL)

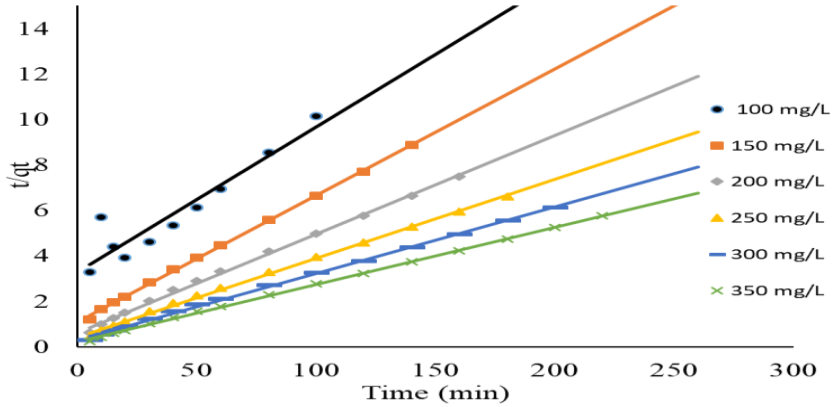


Figure 21: The Pseudo-second-order Kinetic Plot for Adsorption of Direct Black 168Dye onto Mango Leaf Powder (C_0 = 100, 150, 200, 250, 300, & 350 mg/L, W = 0.75 g, V = 100 mL)

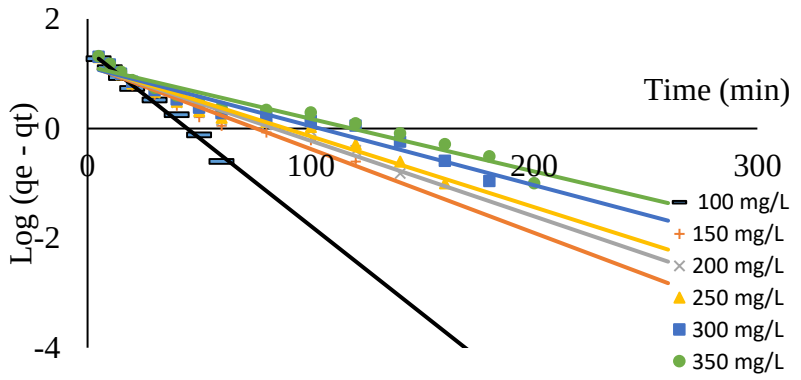


Figure 22: The Pseudo-first-order Kinetic Plot for Adsorption of Direct Black 168Dye onto Mango leaf – activated Carbon (C_0 = 100, 150, 200, 250 mg/L, W = 0.35 g, V = 100 mL)

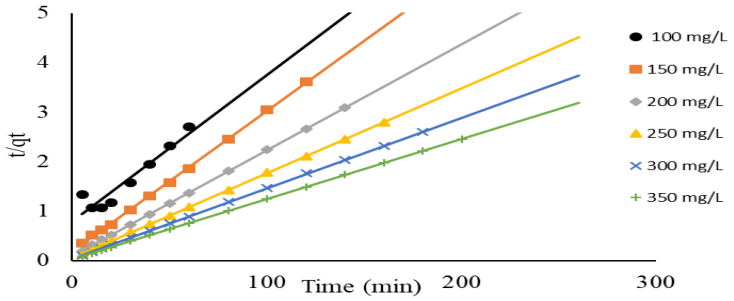


Figure 23: The Pseudo-Second-order Kinetic Plot for Adsorption of Direct Black 168Dye onto Mango Leaf – Activated Carbon (C_0 = 100, 150, 200, 250 mg/L, W = 0.35 g, V = 100 mL)

All the isotherm parameters in table 5 and 6 were calculated from figure 20 to 23.

Table 5: Kinetic Parameters for the Adsorption of Direct Black 168 dye by Mango Leaf Powder

C_0 (mg/L)	Pseudo-first-order model				Pseudo-second-order model			
	$q_{e(exp)}$ (mg/g)	k_1 (min^{-1})	$q_{e(cal)}$ (mg/g)	R^2	$q_{e(exp)}$ (mg/g)	k_2 (g/mg.min)	$q_{e(cal)}$ (mg/g)	R^2
100	10.09	0.0364	11.18	0.9903	10.09	0.0012	15.67	0.8850
150	16.18	0.0246	12.42	0.9979	16.18	0.0028	17.99	0.9993
200	21.59	0.0242	14.60	0.9931	21.59	0.0030	23.09	0.9982
250	27.27	0.0258	18.44	0.9736	27.27	0.0028	28.82	0.9983
300	32.83	0.0219	16.97	0.9948	32.83	0.0028	34.25	0.9988
350	38.30	0.0223	17.81	0.9985	38.30	0.0029	39.68	0.9992

Table 6: Kinetic Parameters for the Adsorption of Direct Black 168 dye by Mango Leaf-Activated Carbon

C_0 (mg/L)	Pseudo-first-order model				Pseudo-second-order model			
	$q_{e(exp)}$ (mg/g)	k_1 (min^{-1})	$q_{e(cal)}$ (mg/g)	R^2	$q_{e(exp)}$ (mg/g)	k_2 (g/mg.min)	$q_{e(cal)}$ (mg/g)	R^2
100	22.38	0.0739	27.25	0.9891	22.38	0.0011	33.78	0.9018
150	33.45	0.0352	14.34	0.9471	33.45	0.0044	35.21	0.9994
200	45.49	0.0318	14.24	0.9542	45.49	0.0052	46.73	0.9999
250	57.38	0.0297	14.08	0.9613	57.38	0.0057	58.14	0.9999
300	69.43	0.0249	13.28	0.9448	69.43	0.0055	69.93	1.0000
350	81.72	0.0221	13.74	0.9518	81.72	0.0053	82.64	1.0000

Limitations of the Study

This study focused primarily on the comparative adsorption performance, equilibrium behaviour and kinetics of MLP and ML-AC. Detailed physicochemical characterization, including BET surface area, pore-volume analysis, pore-size distribution, SEM, FTIR and elemental analysis, was not included in the present adsorption-focused manuscript and is addressed separately. Consequently, interpretations concerning changes in surface properties following activation are presented cautiously and are not used as direct evidence of increased surface area or adsorption-site density.

The thermodynamic parameters (such as ΔG^o, ΔH^o, ΔS^o) were not determined. Consequently, the spontaneity and thermodynamic nature of the adsorption process could not be established from the present experimental data.

Long-term stability and adsorbent reusability were not assessed. This study was limited to laboratory-scale experiments using a single anionic dye, Direct Black 168. The adsorbents - mango leaf powder and its derived activated carbon, were not tested on other dye pollutants or in real wastewater conditions.

CONCLUSION

This study demonstrated the effectiveness of mango leaf powder (MLP) and mango leaf–activated carbon (ML-AC) for the removal of Direct Black 168 dye from aqueous solution. Adsorption efficiency was influenced by pH, initial dye concentration, contact time, and adsorbent dosage, with ML-AC consistently outperforming MLP. Equilibrium data fitted best to the Freundlich model, indicating heterogeneous multilayer adsorption, while kinetic analysis showed that the pseudo-second-order model provided the best fit to the experimental data, suggesting that surface interactions may contribute to the adsorption rate. Under optimized adsorption conditions, ML-AC achieved an optimum removal efficiency of 78.34 %, compared with 75.66 % for MLP. The corresponding experimental equilibrium adsorption capacities were 22.38 mg/g for ML-AC and 10.09 mg/g for MLP at an initial dye concentration of 100 mg/L, while ML-AC reached equilibrium within 80 min, whereas MLP required 120 min under the same conditions. The study demonstrates that both mango leaf powder and mango leaf-derived activated carbon are potential sustainable adsorbents for the removal of Direct Black 168 from aqueous solution, with phosphoric acid activation improving the adsorption performance of the mango leaf powder under the investigated conditions.

This study was limited to laboratory-scale experiments using a single anionic dye, Direct Black 168, the absence of characterization, thermodynamic analysis, long-term stability and adsorbent reusability were not assessed. The adsorbents – mango leaf powder and its derived activated carbon, were not tested on other dye pollutants or in real wastewater conditions. Future studies should optimize H_3PO_4 activation process by systematically investigating acid concentration, impregnation ratio, activation temperature, and activation time to maximize adsorption performance while minimizing chemical and energy requirements. Further studies should also evaluate the thermodynamic parameters of adsorption, adsorbent regeneration and reuse, continuous-flow treatment, and techno-economic feasibility before scale-up for practical wastewater treatment.

ACKNOWLEDGEMENT

The authors express their sincere gratitude to Almighty God and acknowledge all individuals whose support, encouragement, and contributions facilitated the successful completion of this research. Their assistance in various capacities is appreciated.

CONFLICT OF INTEREST STATEMENT

The authors declare that there are no conflicts of interest regarding the publication of this article.

FUNDING ACKNOWLEDGEMENT

This research received no external institutional funding. Financial support was provided privately.

REFERENCES

Adegoke, H. I., Audu, M. F., Bello, M. O., & Olukolatimi, F. (2021). Kinetic and Thermodynamic Adsorption Studies of Methylene Blue onto Zeolite from Aqueous Solution. *Federal*

University Dutsin-Ma Journal of Sciences (FJS), 5(1), 27 – 36.

Adelaja, O. A., Bankole, A. C., Oladipo, M. E., & Lene, D. B. (2019). Biosorption of Hg (II) ions, Congo red and their binary mixture using raw and chemically activated mango leaves. *International Journal of Energy and Water Resources*, 3(1), 1 – 10.

Ali, S., Mehdi, F., & Seyed, A. M. P. (2021). A review on adsorbent parameters for removal of dye products from industrial wastewater. *Water Quality Research Journal*, 56(4), 181-193.

Aminu, I., Gumol, S. M., Ahmad, W. A., & Idris, A. A. (2020). Adsorption Isotherms and kinetics Studies of Congo Red Removal from Wastewater using Activated Carbon Prepared from Jujube Seed. *American Journal of Analytical Chemistry*, 11(1), 47 – 59.

Aragaw, T. A. (2024). A review of Dye Biodegradation in Textile Wastewater, Challenges due to Wastewater Characteristics, and the potential Alkaliphiles. *Journal of Hazardous Materials Advances*, 16, 1 – 20.

Attallah, O. A., Al-Ghobashy, M. A., Nebsen, M., & Salem, M. Y. (2016). Removal of cationic and anionic dyes from aqueous solution with magnetite/pectin and magnetite/silica/pectin hybrid nanocomposites: kinetics, isotherm and mechanism analysis. *Royal Society of Chemistry*, 6(14), 11461-11480.

Bello, O. S., Auta, M., & Ayodele, O. B. (2013). Ackee apple (*Blighia sapida*) seeds: a novel adsorbent for the removal of the Congo red dye from aqueous solutions. The Journal of Chemical Ecology, 29(1), 58 – 71.

Chikri, R., Elhadiri, N., Benchanaa, M., & El Maguana, Y. (2020). Efficiency of Sawdust as Low-Cost Adsorbent for Dyes Removal. *Journal of Chemistry*, 2020(3-4), 1-17. https://doi.org/10.1155/2020/8813420

Crini, G. (2006). Non-conventional low-cost adsorbents for dye removal: a review. *Bioresource Technology*, 97(9), 1061–1085.

Danish, M., & Ahmad, T. (2018). A review on utilization of wood biomass as a sustainable precursor for activated carbon production and application. *Renewable and Sustainable Energy Reviews*, 87, 1–21. https://doi.org/10.1016/j.rser.2018.02.003

Elwakeel, K. Z., Elgarahy, A. M., Elshoubaky, G. A. & Mohammad, S. H. (2020). Microwave assist sorption of crystal violet and Congo Red dyes onto amphoteric sorbent based on upcycled sepia shells. *Journal of Environmental Health Science & Engineering*, 18(1), 35–50. https://doi.org/10.1007/s40201-019-00435-1.

Emmanuel, I.U., Gilbert, U.A., Lora O.O., Olalere, G.A., (2009): Multistage Optimization of the Adsorption of Methylene Blue Dye onto Defatted Carica papaya Seeds. *Chemical Engineering Journal*, 155(3), 567 – 579.

Foo, K. Y., & Hameed, B. H. (2010). Insights into the modeling of adsorption isotherm systems. *Chemical Engineering Journal*, 156(1), 2–10. https://doi.org/10.1016/j.cej.2009.09.013

Gao, J., Zhang, Q., Su, K., Chen, R., & Peng, Y. (2010). Biosorption of Acid Yellow 17 from aqueous solution by non-living aerobic granular sludge. *Journal of Hazardous Materials*, 174(1-3), 215–225.

Garg, V. K., Gupta, R., Yadav, A. B., & Kumar, R. (2003). Dye removal from aqueous solution by adsorption on treated sawdust. *Bioresource Technology*, 89(2), 121–124. https://doi.org/10.1016/s0960-8524(03)00058-0.

Ghoreishi, S. M., & Haghighi, R. (2003). Chemical catalytic reaction and biological oxidation for treatment of non-biodegradable textile effluent. *Chemical Engineering Journal*, 95(1–3), 163–169. https://doi.org/10.1016/s1385-8947(03)00100-1.

Guiza, S., Launay, F., & Bagane, M. (2018). Adsorption of dyes from aqueous solution under batch mode using cellulosic orange peel waste. *Desalination and Water Treatment*, 113, 262 – 269.

Ho, Y.S., & McKay, G. (1999). Pseudo-second-order model for sorption processes, *Process Biochemistry*, 34(5), 451 – 465.

Ibrahim, M. B., & Jimoh, A. (2019). *Mangifera indica* leaves powder for the removal of Rhodamine B.: Isotherm and kinetic studies. *Chemsearch Journal*, 10(1), 71-78.

Idan, I. J., Abdullah, L. C., Choong, T. S. Y., & Jamil, S. N. A. B. M. (2018). Equilibrium, kinetics and thermodynamic adsorption studies of acid dyes on adsorbent developed from kenaf core fiber. *Adsorption Science & Technology*, 36(1–2), 694–712. https://doi.org/10.1177/0263617417715532

Inbaraj, B. S., & Chen, B. G. (2011). Dye adsorption characteristics of magnetite nanoparticles coated with a biopolymer poly (gamma-glutamic acid). *Bioresource Technology*, 102(19), 8868-8876.

Ioannidou, O., & Zabaniotou, A. (2007). Agricultural residues as precursors for activated carbon production—A review. *Renewable and Sustainable Energy Reviews*, 11(9), 1966–2005. https://doi.org/10.1016/j.rser.2006.03.013

Kamga, F. T. (2019). Modeling adsorption mechanism of paraquat onto Ayous (Triplochiton scleroxylon) wood sawdust. *Applied Water Science*, 9(1), 1 – 7. https://doi.org/10.1007/s13201-018-0879-3

Khan, M.M.R., Sahoo, B., Mukherjee, A.K., & Naskar, A. (2019). Biosorption of Acid Yellow-99 using Mango (*Mangifera indica*) Leaf Powder, an Economic Agricultural Waste. *Springer Nature Applied Sciences*, 1(11), 1 – 15.

Khayyun, T. S. & Mseer, A. H. (2019). Comparison of the experimental results with the Langmuir and Freundlich models for copper removal on limestone adsorbent. *Applied Water Science*, 9(8), 1 – 8. https://doi.org/10.1007/s13201-019-1061-2.

Kolawole, S. A., Tijjani-Garba, H., & Omoniyi, A. O. (2022). Adsorption Behaviour of Methylene Blue Dye on Eggshell

Extracted Chitosan and Carbonized Date-Pits as Adsorbents. *Journal of the Chemical Society of Nigeria*, 47(2), 272 –283.
Lagergren, S. (1898). Zur theorie der sogenannten adsorption geloster stoffe. *Kungliga Svenska Vetenskapsakademiens Handlingar*, 24, 1–39.

Lizada, C. (1993). Mango. In Seymour, G. B., Taylor, J. E., & Tucker, G. A. (Eds.), *Biochemistry of Fruit Ripening* (pp. 255–271). *Springer*. DOI: https://doi.org/10.1007/978-94-011-1584-1_8.

M'Hamdi, A. I., Kandri, N. I., Zerouale, A., Blumberga, D., & Gusca, J. (2016). Treatment and physicochemical characterization of red wood sawdust. *Energy Procedia*, 95, 546–550.

Malik, P. K. (2003). Use of activated carbons prepared from sawdust and rice-husk for adsorption of acid dyes: A case study of Acid Yellow 36. *Dyes and Pigments*, 56(3), 239–249. https://doi.org/10.1016/S0143-7208(02)00159-6

Matos, J., Nahas, C., Rojas, L., & Rosales, M. (2011). Synthesis and characterization of activated carbon from sawdust of Algarroba wood. 1. Physical activation and pyrolysis. *Journal of Hazardous Materials*, 196, 360–369.

Murugan, T., Ganapathi, A., & Valliappan, R. (2010). Removal of Dyes from Aqueous Solution by Adsorption on Biomass of Mango (*Mangifera Indica*) Leaves. *E-Journal of Chemistry*, 7(3), 669-676.

National Center for Biotechnology Information. (2026). PubChem compound summary for Direct Black 168 (CID 102058859). PubChem. https://pubchem.ncbi.nlm.nih.gov/compound/102058859

Neag, E., Moldovan, A., Babalau-Fuss, V., Torok, A., Cadar, O., & Roman, C. (2019). Kinetics, Equilibrium and Phytotoxicity Studies for Dye Removal by Low-Cost Natural Activated Plant-Based Carbon. *Acta Chimica Slovenica*, 66(4), 850-858.

Neme, I., Gonfa, G., & Masi, C. (2022). Activated carbon from biomass precursors using phosphoric acid: A review. *Heliyon*, 8(12), e11940. https://doi.org/10.1016/j.heliyon.2022.e11940

Nizam, N.U.M., Hanafiah, M.M., Mahmoudi, E., Halim, A.A., & Muhammad, A.W. (2021). The removal of Anionic and Cationic Dyes from an Aqueous Solution using Biomass-based Activated Carbon. *Scientific Reports*, 11(1), 8623. https://doi.org/10.1038/s41598-021-88084-z

Ojedokun, A.T., & Bello, O.S. (2017). Kinetic Modeling of Liquid-Phase Adsorption of Congo Red Dye using Guava Leaf-base Activated Carbon. *Applied Water Science*, 7(4), 1965 – 1977.

Piccin, J. S., Vieira, M. L. G., Gonçalves, J. O., Dotto, G. L., & Pinto, L. A. A. (2009). Adsorption of FD&C Red No. 40 by Chitosan: Isotherms Analysis. *Journal of Food Engineering*, 95(1), 16–20.

Salleh, M. A. M., Mahmoud, D. K., Karim, W. A. W. A., & Idris, A. (2011). Cationic and anionic dye adsorption by agricultural solid wastes: a comprehensive review. *Desalination*, 280(1–3), 1–13. https://doi.org/10.1016/j.desal.2011.07.019.

Sangoremi, A. A. (2025). Adsorption Kinetic Models and their Applications: A Critical Review. *The International Journal of Research and Scientific Innovation (IJRSI)*, 12(5), 245 – 258. DOI: https://doi.org/10.51244/IJRSI.2025.120500019

Santhi, T., Manonmani, S., Vasantha, V. S., & Chang, Y. T. (2016). A new alternative adsorbent for the removal of cationic dyes from aqueous solution. *Arabian Journal of Chemistry*, 9(1), 466-474.

Satish, P., Sameer, R., & Naseema, P. (2012). Removal of methylene blue, a basic dye from aqueous solutions by adsorption using mango (*Mangifera indica*) leaf powder. *Environmental Science*, 7(7), 239-250.

Shining, V.P.T., & Helen, D. (2022). Kinetic and Equilibrium Studies of Methyl Orange Removal from Aqueous Solution by Adsorption on Activated Rubber Sawdust. *International Journal of Advanced Research in Science, Communication and Technology*, 2(2), 828 – 834.

Sirajoa, L., & Zainia, M. A. A. (2023). Adsorption of water pollutants using H_3PO_4-activated lignocellulosic agricultural waste: A mini review. Toxin Reviews, 42(1), 349–361. https://doi.org/10.1080/15569543.2022.2062775

Skoog, D.A., Holler, F.J., & Crouch, S.R. (2014). Principles of Instrumental Analysis (7th ed., pp. 169 – 174). Cengage Learning.

Son, D. H. B., Mai, V. Q., Du, D. X., Phong, N. H., & Khieu, D. Q. (2016). A study on Astrazon Black AFDL dye adsorption onto Vietnamese diatomite. *Journal of Chemistry*, 2016(1), 1–11. https://doi.org/10.1155/2016/8685437.

Uddin, M. T., Rahman, M. A., Rukanuzzaman, M., Islam, M. A. (2017). A potential low-cost adsorbent for the removal of cationic dyes from aqueous solutions. *Applied Water Science*, 7(6), 2831-2842.

Yunus, M. M., & Nuhu, A. H. (2020). Thermodynamic Study of Congo red Dye Adsorption using Rice Husk Activated Carbon. *International Journal of Research and Scientific Innovation (IJRSI)*, 7(3), 124 – 128.

Zewde, D., & Geremew, B. (2022). Removal of Congo Red using *Vernonia amygolalina* leaf powder: Optimization, Isotherm, Kinetics, and Thermodynamics Studies. *Environmental Pollutants and Bioavailability*, 34(1), 88 – 101.

Zuo, S., Yang, J., & Liu, J. (2010). Effects of the heating history of impregnated lignocellulosic material on pore development during phosphoric acid activation. Carbon, 48(11), 3293–3295. https://doi.org/10.1016/j.carbon.2010.04.042

©2026 This is an Open Access article distributed under the terms of the Creative Commons Attribution 4.0 International license viewed via https://creativecommons.org/licenses/by/4.0/ which permits unrestricted use, distribution, and reproduction in any medium, provided the original work is cited appropriately.